23rd ABCM International Congress of Mechanical Engineering
December 6-11, 2015, Rio de Janeiro, RJ, Brazil

SCHEFFLER PARABOLOIDAL CONCENTRATOR IMAGE ANALYSIS

Erick Alfred Dib
Flávio Augusto Sanzovo Fiorelli
Escola Politécnica, University of São Paulo, Mechanical Engineering Dept.
edib@usp.br; fiorelli@usp.br

Abstract. *The purpose of this work is to improve the design of the receivers used in the Scheffler concentrators to avoid losses of energy at the entrance of the thermal radiation absorbers. The Scheffler concentrator is a paraboloidal solar concentrator that works in a two-axes track system; thus maintaining the focal image fixed on its stopped absorber according to the variation of the solar declination and azimuth. The image formed by the Scheffler concentrator is presented. The reflector has elliptical profile and its geometry is defined by the lateral section of a paraboloid. Rim angles at equinox are approximately 49.6 and 109.6 degrees from the paraboloid axis. The tracking system for adjusting it according to the variation of the solar declination causes these rim angles to change. An analysis of the effects of these variations on the image of the focus, the aperture area in relation to the Sun, and the concentration ratio is performed. The variation of the rim angles was found to cause variations on the size of the focal image of Scheffler reflectors on two axes, and these variations differ among them. In the tropical region, the simulations indicate that aperture area and concentration ratio vary from 0,62 m*^{2} *to 1,369 m*^{2} *and from 2499 to 6678 respectively.*

Keywords: *Solar Energy, Scheffler Concentrator, Imaging, Focusing, Optical Device Fabrication*

Nomenclature

A	Area [m^2]
C	Concentration ratio [dimensionless]
x, y, z	Position of some point over x, y or z axis [m]
Special characters	
θ	Half angle of variation of solar radiation beam incidence regarding solar disc or concentration imperfections [º]
δ	Solar declination [º]
ϕ	Rim angle [º]
φ	Variable rim angle [º]
Subscripts	
A, B	Referring to point A or B
axis	Referring to the axis of daily tracking system
b	Variations by the building of solar concentrator
c	Variations by the solar concentrator
down	Downside of the focus point
l	Referring to point L
m	Imperfections of the mirror
s	Ellipsis area or Scheffler area
x, y	Width over the x or y axis
up	Upside of the focus point

1. INTRODUCTION

The Scheffler concentrator is a paraboloidal solar concentrator developed by physicist Wolfgang Scheffler in the 1980s (Oelher and Scheffler, 1994). It maintains the image of the focus fixed on a given place. The surface of the reflector consists of the lateral section of a paraboloid, thus conferring the frame an elliptical shape, although the surface is a paraboloid. The focus keeps positioned in front of the reflector, since the directrix plane is the one below. There is no shadow over the parabolic reflector due to the receiver. That occurs to some types of paraboloidal solar concentrators.

The image of the focus stays on a fixed place at the stopped receptor that can be separated from the structure of the Scheffler concentrator. This is possible because the track system of the Scheffler concentrator works in two axes. One is parallel to the polar axis and maintains the image of the focus fixed according to the hour solar angle variations; and for that, it can be directed only to the North and South Poles. The other axis is directed to the east – west to maintain the image of the focus fixed in respect to the solar declination variations. Thereby, the movement of the focus is only possible by the effect of daily tracking systems. The image of the focus makes the rotation with the reflector, on the same axis. The image appears to rotate. The center of this rotation is the axis of daily rotation of the solar concentrator. In this way, the receptor can be stopped.

With these characteristics, the receivers described by many authors show the large array of possibilities opened by the Scheffler concentrator. For example, a kitchen provided with a Scheffler concentrator with 7 m^2 of ellipse area, A_s, was built (Oelher and Scheffler, 1994). The rays reflected by this solar concentrator went through the window and were reflected by a secondary reflector. Then, the solar rays reached the receptor. The receptor had a support for some vessels with volumes between 80 and 100 liters. The absorber was at the bottom of the vessels and the second reflector was below the vessel. The receptor was not connected to the structure of the concentrator. It was placed in a shadowed place and thermally isolated so that it could be put on fire, for cooking in the traditional method, when there was not beam radiation over the reflector. According the authors, the power verified at the focus image of the Scheffler reflector was 2.1 kW for 730 W/m^2 of beam irradiation. The experiments were carried out in Sudan, in April, and the aperture area, A_{ap}, was 4.7 m^2. The power verified at the cooker was 1.4 kW. The losses because of the second reflector were 60%. The diameter of the focal image was 0.6 m, and the maximum temperatures achieved at the bottom were between 200 and 350°C. Patil et al. (2011) and Schapers (2009) carried out other studies with similar configurations, changing the sizes of both the Scheffler concentrator and the cocking pot.

In India, Scheffler (2006a) developed a solar crematorium with heating system supplied by the Scheffler concentrator. According to the author, the system was built with a reflector area, $A_{s,}$ of 3.4 m^2, reaching the power of 1 kW and temperatures higher than 800°C. The receptor was the cremation chamber and the absorber was its interior. At the focal image place there was a circular shape with an orifice in the center, measuring 80 mm in diameter, from where the concentrated solar radiation entered the chamber. The concentration ratio was about 676.

In Germany, Tyroller (2006) developed a hybrid autoclave, provided with Scheffler fixed focus concentrator, for rural hospitals. The cylindrical absorber for the receptor was an iron block with mass of 260 kg and an internal serpentine. The image of the focus was projected on one of the cylinder bases. In the serpentine, steam was generated and conducted into a sterilized chamber of 76 liters by a closed water-steam cycle. In cloudy days, the source of energy was the traditional ones (gas and electrical boilers). The sterilizing temperature at atmosphere pressure is 121°C. According to the author, the idea was to improve efficiency and to supply a storage system through pressurized steam. The superheated vapor achieved temperatures higher than 500°C, and the author verified that for most of the day, the sterilization was carried out.

Other types of receiver were developed for Scheffler reflectors. The solar distiller system, developed by Chandak and Somani (2009) was provided with two Scheffler concentrators with A_s = 16 m^2 each. Both receivers seemed a disc, each, a flattened cylinder with base diameters of 400 mm. The energy of the focal image was absorbed by one of the bases, making this base the absorber. By cycled periods, salty water entered the cylindrical absorbers and the heat from the absorber was conducted to the fluid, and steam left from one of receivers.

In India, solar evaporators were developed and installed in many solar kitchens and in the industry by Gadhia (2009) and Lukhi (2009), respectively. Both systems work with receivers similar to the ones proposed by Chandak and Somani (2009), but two Scheffler concentrators were installed, one for each receiver. One reflector was directed to the South Pole, while the other, to the North Pole. They were placed face to face with the receiver in a space in which both images could be focused on the opposite side of the same receiver. Each image was incident/reflected on one of the flattened cylinder bases connected to a steam tube that conducted it through the system.

Since the first publications concerning the Scheffler concentrator, many other configurations of receivers than those reported were developed. However, thermal losses can occur due to the incorrect sizing of the region in which the focal image reaches the receiver; thus, making improvements in the efficiency of the receivers necessary. This paper analyses the image formed by the Scheffler reflector in the lateral and top planes to allow proper sizing of the absorbers and to increase the efficiency of the receivers designed for the Scheffler concentrators. The incidence angle modifier is also analyzed, and a mathematical model based on optical characteristics and analytical geometry is proposed.

2. THE SCHEFFLER CONCENTRATOR

The geometry of the Scheffler reflector is described as the lateral section of a paraboloid (Scheffler, 2006b). It is inclined at 43.23° just at equinox. As it works with a tracking system on two axes, the image of the focus stays at the same place, in front of the mirror, throughout the year. Therefore, it is possible to create the image in the shadow.

The targeting of the Scheffler concentrator is possible for only two positions: the North or the South. The Scheffler concentrator directed to the North, SCDN, means that the mirror reflects the solar energy to the North, the direction of the focal image, analogously to the Scheffler concentrator directed to the South (SCDS). Figure 1 shows the lateral view, or the *xy* coordinate plane view.

The scheme in Fig. 1 shows that the axis of the daily tracking system works parallel to the polar axis, and perpendicularly to solar rays just at equinox. The daily tracking system goes through the center of the mirror of the reflector throughout the year. It also illustrates how it is possible to fix two Scheffler reflectors in one receiver, as explained by some works in the previous section.

The rim angles of the Scheffler concentrator can be defined by the angle formed between the axis of the parabola (*y* coordinate) and its extreme points, A and B, in the *xy* coordinate. The other rim angle is located between the *x* coordinate and point M, in the *xz* coordinate illustrated in Fig. 2. Just at equinox, the rim angles of all Scheffler reflector are always ϕ_a = 49.59°, ϕ_{axis} = 90°, ϕ_b = 109.62° ϕ_m = 26.96°. The view of this coordinate system shows the aperture plane of the Scheffler concentrator in relation to the Sun.

The seasonal tracking system works on the axis parallel to the *z* coordinate, as shown in Fig. 2. In the *xy* coordinate (Fig. 1), this axis enters perpendicularly at the point near P. It is fixed on the reflector at two points z_m. The action of the seasonal track system changes the parabola profile and, consequently, the size of the aperture area of the concentrator in relation to the Sun (Munir et al. 2010).

If this solar concentrator has fixed focus on the desired place, the reflector slope changes according to the variation of the solar declination. The value of the slope change is half of the value of the solar declination. Fig. 3 illustrates the extreme conditions of the parabola shape. In other words, it shows the parabolic profile at equinox and both solstices for both Scheffler concentrator positions.

There is one point on the mirror that is also fixed (point C), which is close to the center of the mirror and coincident with point x_m on the parabola line. The distance between point C and the focus is fixed. The *y* coordinate always points to the Sun. The *x* coordinate coincides with the North-South coordinate just at equinox. This coordinate varies at the same value as the solar declination, and coincides with the horizon at latitude 0°. Therefore, this coordinate has the same slope as the latitude of where it is installed.

The slope varies in the same way for both systems with one receiver for two concentrators. From Fig. 3 the SCDN is found to be at the highest parabola in the summer solstice in the North hemisphere, while the SCDS is at the lowest parabola. Consequently, the larger the latitude, the greater the similarity that one concentrator seems to work in a lying position, while the other is in a standing position.

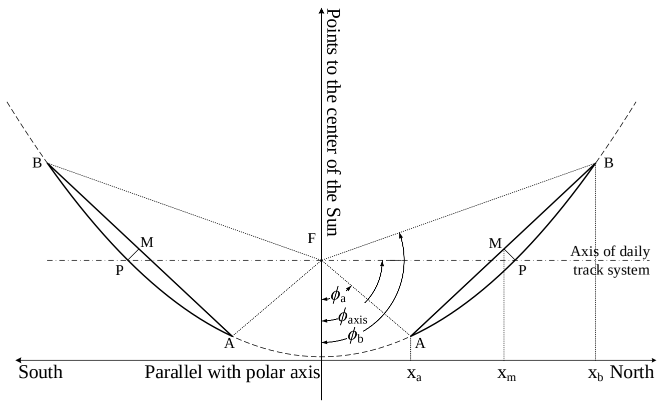

Figure 1. Lateral view of the Scheffler concentrator in *xy* coordinates.

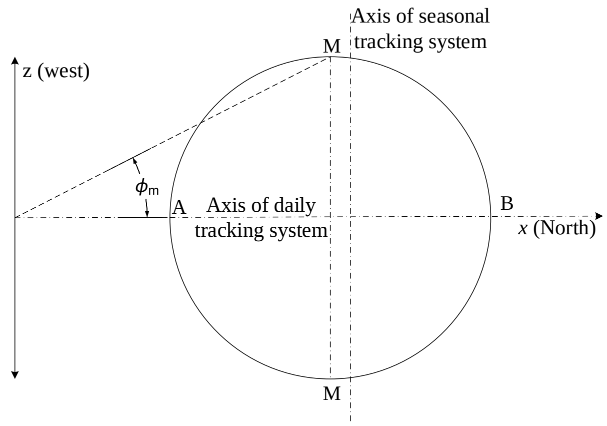

Figure 2. Upside view of the Scheffler concentrator in *xz* coordinates.

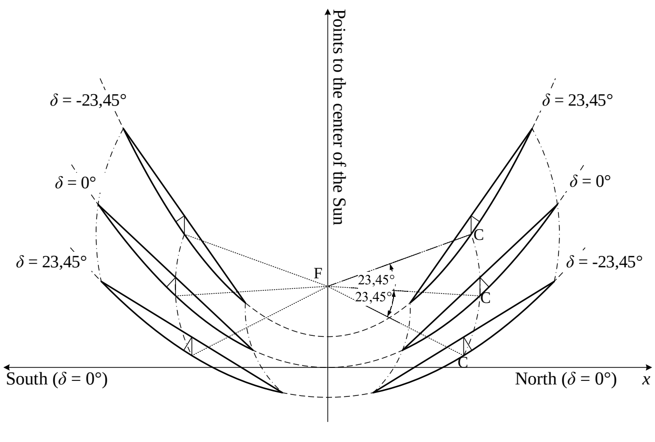

Figure 3. Lateral view of the Scheffler reflector at equinox and both solstices (*xy* coordinates).

3. IMAGE FORMED BY THE SCHEFFLER CONCENTRATOR

To better understand the energy flux from the concentrator to the receivers, provided by the solar radiation beam reflected from the Scheffler reflector that are concentrated at the focal place of the receiver, it is necessary to understand how the concentrator operates and forms the image.

Duffie and Beckman (2006) present an analysis about a linear imaging concentrator that can be also applied to paraboloid solar concentrators using the same analytical method, regardless of the different considerations of the Scheffler concentrator, such as the rim angles in two points of view and the mechanism of incidence angle modifier.

The Scheffler concentrator imaging tends to an ellipsis that has four semi axes, or two widths (W) on the y and z coordinates. First, the W_y and W_z were studied separately. The W_y was analyzed in the xy coordinate view, as illustrated in Fig. 4, while the W_z, under xz, shown in Fig. 5, with the help of Fig. 4. Both axes were analyzed together to know how the change in the focal image is due to the solar declination.

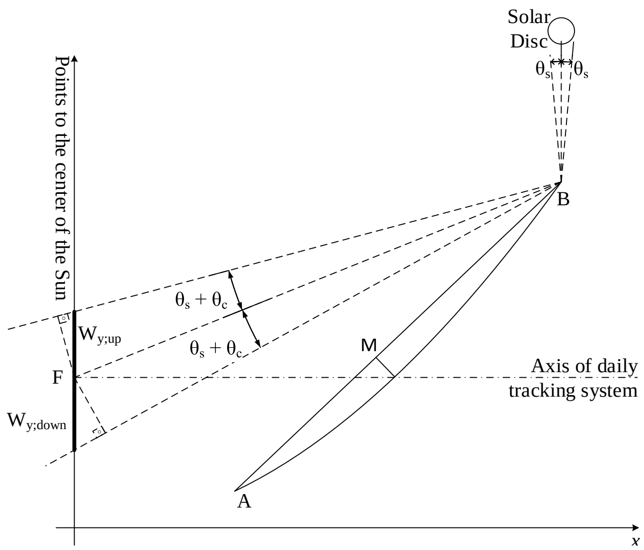

Figure 4. Reflection of the infinitesimal area on the xy plane.

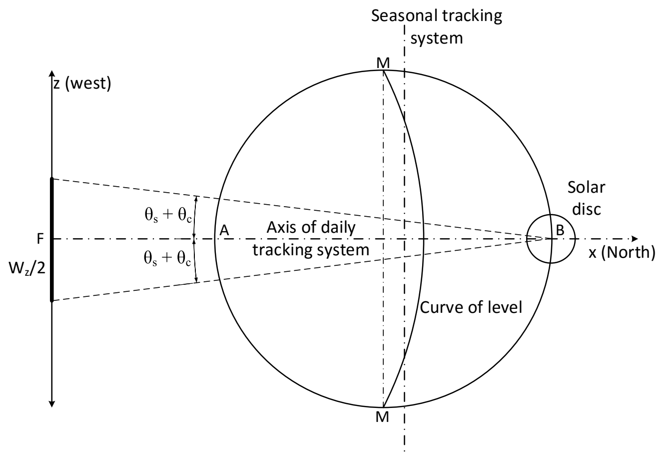

Figure 5. Reflection of the infinitesimal area on the xz plane.

First, note that the Sun is not a point but a disc, which emits the beam radiation to the mirror of the Scheffler concentrator. An infinitesimal area of the reflector can be used to know how the reflection is. Then, if the source of radiation is a disc emitting to an infinitesimal area, the solar rays became cones with an angle of $2\theta_s$. The value of θ_s (the angle between a line from earth to the center of the Sun and other line from Earth to the edge of the solar disc) is approximately 0.27°. In this sense, the infinitesimal area of a perfect concentrator would also reflect cones with $2\theta_s$ angles. However, in practical situations, imperfections related to the mirror and to the structure of concentrator increase the angle of the cone reflected. If an individual analysis would be carried out, in which one beam of light was incident, the imperfections due to the mirror would reflect a cone and the imperfections due the structure would cause a deviation, but it could also be considered a cone. The angle of these cones would be $2\theta_m$ and $2\theta_b$, respectively. Summing that, only concentrator imperfections can be considered, θ_c, since:

$$\theta_c = \theta_m + \theta_b \tag{1}$$

Figure 4 illustrates the solar disc emitting to an infinitesimal area, at point B of the Scheffler concentrator, with a cone angle of $2\theta_s$ and reflecting another cone with an angle of $2(\theta_s+\theta_c)$. In a 2-D drawing the cone becomes a triangle. The central line of this triangle achieves the focal point of the parabola. A perpendicular line to the border of the triangle was created from the focus for both sides. There are four triangles to estimate the image in the y axis coordinate, two for semi axis above the focal point and two for the one below. The width of image on the y axis is defined by:

$$W_y = W_{y,up} + W_{y,down} \tag{2}$$

The analysis of the image formation over the xz plane of the coordinate is represented by the scheme in Fig. 5 used to deduce the equation of W_z. An infinitesimal area also on point B produces the largest projection W_z on the other side of the axis of the daily tracking system.

As observed in Fig. 5, the triangle of the optical cone varies with the solar declination but the angle ($\theta_s+\theta_c$) shown is just a representation according to the real distance. The largest distance between reflectors is in between points B and F. Therefore, the optical cone from point B forms the largest image W_z. If any point on the rim is chosen, different from B, the aperture of the projection of the optical cone will decrease up to point A, the smallest distance.

3.1 Angle Incidence Modifier

The variation of solar declination changes the sizes of the image produced by the Scheffler concentrator. Regarding the operation of the seasonal tracking system, changes occur on the rim angles of the reflector. In the place where the Scheffler concentrator and its receiver are installed, points F and C remain in the same place in relation to the ground. The axis of the daily tracking system also remains in place, but angled at the same degree of the local latitude to achieve parallelism to the polar axis of the Earth.

In order to compose Fig. 3 and the other figures that explain the movements of the Scheffler concentrator, the beam solar radiation leaving the center of the Sun was placed coinciding with the *y* axis, thus, turning the *xy* axes coordinate static to facilitate the explanation of the parabola change.

Axis W_y of the image is always perpendicular to the axis of the daily tracking system. Fig. 6 illustrates how the axis of the daily tracking system interacts with the solar declination and W_y. Furthermore, angles ϕ_a and ϕ_b of the reflector also change by the action of the seasonal tracking system. The effect observed is the change in size of W_y and W_z.

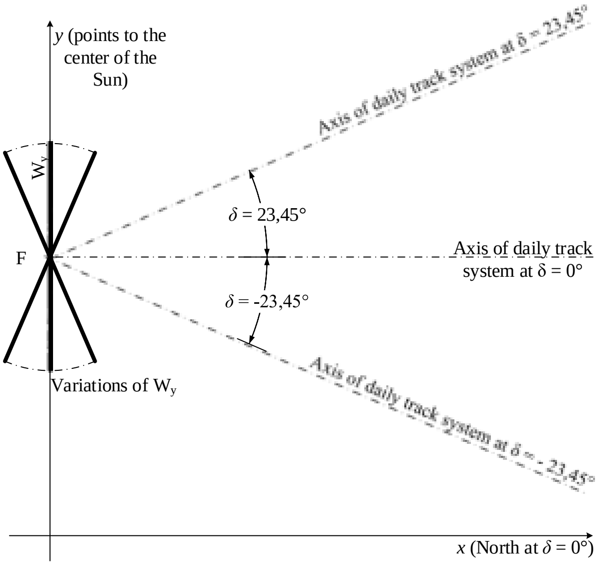

Figure 6. Variation of the projections of W_y according to the solar declination.

The equations that define the sizes of $W_{y;up}$ and $W_{y;down}$ considering the variations in declination from an infinitesimal area at point A, at day *n* and based on parameter *x* of Fig. 3 are

$$W_{y;up;A} = \frac{x_{A;n} \sin\left(\theta_s + \theta_c\right)}{\sin\left(\phi_{A;n}\right)\cos\left[\phi_{axis;n} - \phi_{A;n} + \left(\theta_s + \theta_c\right)\right]} \tag{3a}$$

$$W_{y;down;A} = \frac{x_{A;n} \sin\left(\theta_s + \theta_c\right)}{\sin\left(\phi_{A;n}\right)\cos\left[\phi_{axis;n} - \phi_{A;n} - \left(\theta_s + \theta_c\right)\right]} \tag{3b}$$

and the same from an infinitesimal area at point B

$$W_{y;up;B} = \frac{x_{B;n} \sin\left(\theta_s + \theta_c\right)}{\cos\left(\phi_{B;n} - \phi_{axis;n}\right)\cos\left[\phi_{B;n} - \phi_{axis;n} - \left(\theta_s + \theta_c\right)\right]} \tag{4a}$$

$$W_{y;down;B} = \frac{x_{B;n} \sin\left(\theta_s + \theta_c\right)}{\cos\left(\phi_{B;n} - \phi_{axis;n}\right)\cos\left[\phi_{B;n} - \phi_{axis;n} + \left(\theta_s + \theta_c\right)\right]} \tag{4b}$$

Eqs. (3a) and (3b) can be used to calculate W_y from any infinitesimal area below the axis of the daily tracking system at any day n. The same considerations can be taken into account for any infinitesimal area above the axis of the daily tracking system, Eqs. (4a) and (4b).

The equation that defines the largest size of W_z, considering the angle incidence modifier is

$$W_{z;b} = 2\frac{y_{b;n} - y_f}{\sin\left(\varphi_{B;n} - 90\right)}\tan\left(\theta_S + \theta_c\right) \tag{5}$$

4. TRENDS AND RESULTS

A simulation of the variations in W_y and W_z, with the variation in δ, was performed using the Equation Engineering Solver (EES), considering the Scheffler reflector with A_{ap} = 1 m^2 at equinox.

The infinitesimal area at point B was observed to produce greater W_y, while from point A both sides of W_y increase with solar declination ($W_{y;up;A}$ increases from 3.46 to 5.37 mm and $W_{y;down;A}$ from 3.44 to 5.33 mm). The semi axes from point B decrease with less intensity but with greater value ($W_{y;up;B}$ decrease from 9.03 to 8.47 mm and $W_{y;down;B}$, from 9.06 to 8.51 mm). The variation in W_y for SCDN is shown in Fig. 7, which also shows the variation in W_z from 15.37 to 17.50 mm at the solstices.

The effect of the variations of W_y and W_z on the areas of image produced by SCDN and SCDS, with aperture at equinox of 1 m^2 to the Sun, are presented in Fig. 8. Both, Wy and Wz, curves are symmetric to n. The maximum and minimum limits on the size of the focal area occurs at solstices. For a SCDS, the largest image area calculated was 248.6 mm^2 in the Capricorn Solstice and the smallest A_f, for ideal concentrators, was 205 mm^2 in the Cancer Solstice. For the SCDN, the result is the same, but inversely.

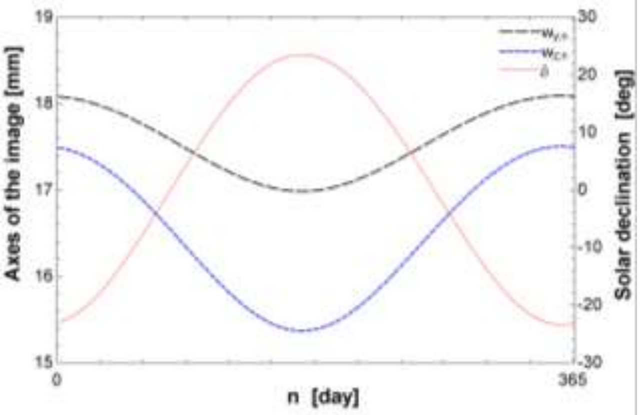

Figure 7. Variations in W_y and W_z with SCDN solar declination

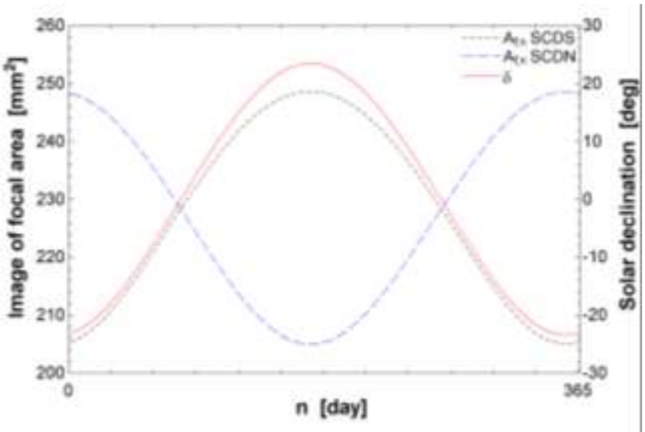

Figure 8. Variations in the focal image area of SCDN and SCDS

In solstice at the Tropic of Cancer, A_{ap} is 1.37 m^2 for SCDN and 0.62 m^2 for SCDS. In the solstice at the Tropic of Capricorn the opposite occurs. This variation is highly significant, and Fig. 9 shows that for SCDNs installed in the South hemisphere of the Earth in the winter, the Scheffler concentrator can deliver more energy to the receiver than in the summer. The same effect happens for SCDS installed in the North hemisphere. Adverse effects occur with the replacement of the Scheffler concentrators in each hemisphere.

Fig. 10 presents a representative sketch of the external boundaries of the imaging Scheffler reflector at the three limits of the solar declination, in both solstices and equinox. The image formed has an elliptical contour with variations in size. Taking SCDS into account, the larger external boundary is the image of the Cancer Solstice, while the smaller external boundary is formed at the Capricorn Solstice. The middle size is formed at both Equinoxes. The considerations for the SCDN are the inverse.

Due to the variation in size of the aperture area and the focal image, the concentration ratio of the Scheffler reflectors also have the variations. The general definition of concentration ratio can also be used for this type of solar concentrator

$$C = A_{ap} / A_f \tag{6}$$

Figure 11 shows the variation range of the concentration ratio for a single SCDN, single SCDS and both pointing to the opposite sides of the same receiver.

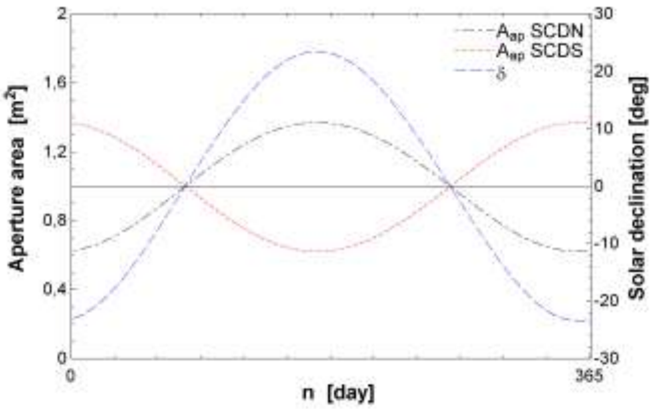

Figure 9. Variation of the aperture area of SCDN and SCNS.

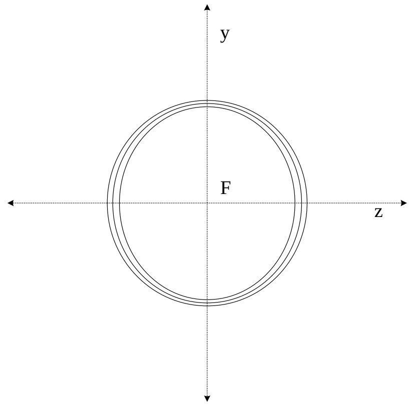

Figure 10. Image of the focus at equinox and both solstices.

Applications using two Scheffler reflectors in one receiver with focus incidence on opposite sides were considered in Fig. 11 by summing the aperture and the focal images areas. The concentration ratio shows better equilibrium when compared to systems using one Scheffler concentrator. The maximum and minimum values of concentration ratio for these systems are 4389 and 4387 with standard deviation of 3.235. Fig. 12 illustrates the concentration ratio for imperfect Scheffler concentrators with different θ_c. The greater θ_c results in lower variation in the concentration ratio, and consequently, the lower flow per unit of area of solar energy in the image of the focus.

The results of analysis for SCDN features at both Solstices and Equinox are shown by Table **1**. Although some of these values were discussed above, Scheffler ellipsis area, aperture area, concentration ratio, parabola angles, image axes, and parabola profile equation were also exposed by Table **1**. The parabola rim angle variations were also illustrated by Fig. 1. The column of equations of parabola profiles represents the three parabolas indicated by Fig. 3. The area of image can be calculated by equation (6) or by ellipsis area equation using the values of W_y and W_z. To know the same values for SCDS it is only change the sign of solar declination in first column of Table **1**, that is, the results for δ = 23.44° became those for δ = - 23.44°, and δ = - 23,44° became δ = 23,44°.

Table 1 Variations values from SCDN (A_{ap} = 1 m^2 at equinox) at both Solstices and Equinox.

δ [°]	A_s [m^2]	A_{ap} [m^2]	C	ϕ_a [°]	ϕ_b [°]	ϕ_{axis} [°]	ϕ_m [°]	W_y [mm]	$W_{y;up}$ [mm]	$W_{y;down}$ [mm]	W_z [mm]	Equation
-23.44	1.08	0.62	2499	78.6	127.6	113	23.1	18.09	9.03	9.06	17.50	$y=0.68x^2+0.22$
0	1.37	1	4385	49.6	109.6	90	27	17.56	8.76	8.79	16.54	$y=0.42x^2$
23.44	1.61	1.37	6678	23.1	91.2	66	33.7	16.98	8.47	8.51	15.37	$y=0.31x^2-0.22$

Each application needs to be carefully studied before deciding the orientation of the Scheffler concentrator. The solar area reflected from the reflector to the receiver varies more than once between the extremes of solar declination,

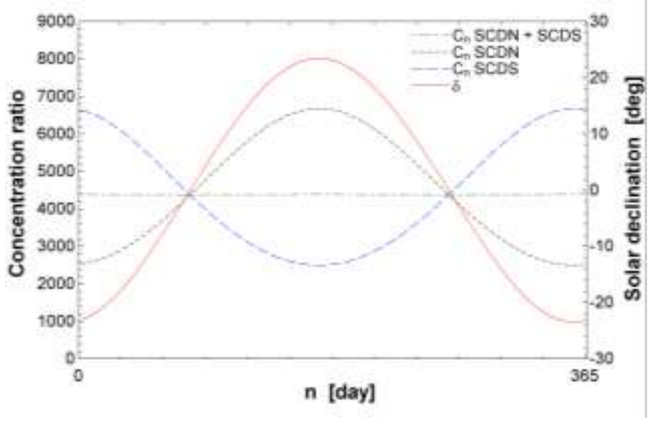

Figure 11. Variations in the concentration ratio of SCDN, SCDS, and in both.

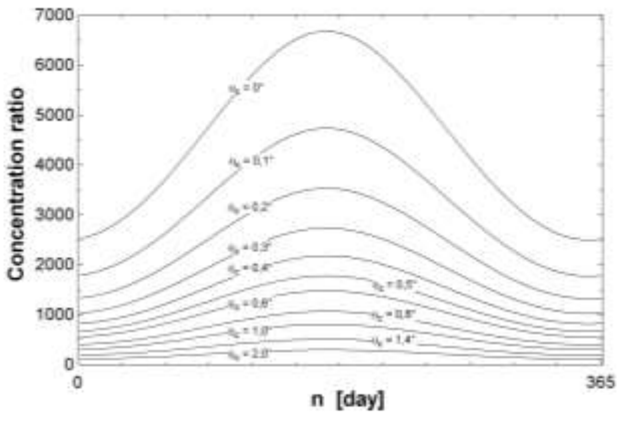

Figure 12. Variations in the concentration ratio of imperfect Scheffler concentrators.

and the concentration ratio varies more than twice a year.

5. CONCLUSION

The results were achieved by using mathematical and optical laws. The application of the equations of W_y and W_z define the angles of deviations of the solar rays reflected from the Scheffler concentrator, the size of the image and the variations in the image formed during the year. The variations of the aperture area and concentration ratio of the Scheffler reflectors were also shown. The image size from the Scheffler concentrator was found between 248.6 mm^2 and 205 mm^2, for A_{ap} = 1 m^2 at equinox. The variation in the A_{ap} was between 0.62 m^2 and 1.37 m^2 at both Solstices. These results suggest that there are significant variations in the energy flow in the receiver and a careful study on energy demand requirements for the given system must be performed.

For SCDN, the concentration ratios were found to be 2499 and 6678 for a perfect reflector at, respectively, the Capricorn and the Cancer solstices. For SCDS, the values are in the reverse order. Regarding the consideration of systems with two Scheffler concentrators, the results showed that these variations can be minimized and the supply of energy in the receiver can be better equalized during the year. The concentration ratio of systems with both Scheffler concentrators, the variations were between 4389 and 4387 with standard deviation of 3.235. However, the image from each Scheffler concentrator is formed on each side of the receiver. Consequently, the variation of each image will be the same as that the receivers with only one concentrator. To minimize the effect of the variations in image, a second concentrator could be designed at the entrance of the concentrated solar radiation into receiver.

To better predict the energy flow and the boundary conditions in the imaging of the Scheffler concentrator, an analysis with Ray Tracing method is suggested. However, continuous study to enhance the efficiency of the receivers for Scheffler reflectors is needed, besides the analysis presented herein.

6. ACKNOWLEDGEMENTS

The authors acknowledge CAPES and PPGEM-USP (-Graduate Program in Mechanical Engineering at the University of São Paulo) for supporting this research.

7. REFERENCES

Chandak, A. and Somani, S.K., 2009. “Design of multistage evaporators for integrating with Scheffler solar concentrators for food processing applications”. In *International Solar Cooker Conference 2009,* paper n^o. 13, Indore, India <http://www.solare-bruecke.org>.
Duffie, J.A. and Beckman, W.A., 2006. *Solar Engineering of Thermal Processes*, John Wiley & Sons, 3rd ed.
Gadhia, D., 2009. “Parabolic solar concentrator for cooking and food processing”. In *International Solar Cooker Conference 2009,* paper n^o. 28, Indore, India <http://www.solare-bruecke.org>.
Lukhi, G., 2009. “Food processing through solar energy”. In *International Solar Cooker Conference 2009,* paper n^o. 57, Indore, India <http://www.solare-bruecke.org>.
Munir, A., Hensel, O. and Scheffler, W., 2010 “Design principle and calculations of a Scheffler fixed focus concentrator for medium temperature applications,” *Solar Energy*, vol. 84, p. 1490-1502.
Oelher, U. and Scheffler, W., 1994. “The use of indigenous materials for solar conversion,” *Solar. Energy Materials and Solar Cells*, vol. 33, p. 379-387.
Patil, R.J., Awari, K.G., and Singh, M.P., 2011. “Experimental analysis of Scheffler reflector water heater,” *Thermal Science*, vol. 15(3), p. 599 - 604.
Schapers, G., 2009. “Agave syrup production - a sweet tradition goes solar”. In *International Solar Cooker Conference 2009,* paper n^o. 25, Indore, India <http://www.solare-bruecke.org>.
Scheffler, W., 2006a. “Development of a solar crematorium”. In *International Solar Cooker Conference 2006,* paper n^o. 22, Granada, Spain <http://www.solare-bruecke.org>.
Scheffler, W., 2006b. “Introduction to the revolutionary design of Scheffler Reflectors”. In *International Solar Cooker Conference 2006,* paper n^o. 21, Granada, Spain <http://www.solare-bruecke.org>.
Tyroller, M., 2006. “Solar steam sterilizer for rural hospitals”. In *International Solar Cooker Conference 2006,* paper n^o. 34, Granada, Spain <http://www.solare-bruecke.org>.

8. RESPONSIBILITY NOTICE

The authors are the only responsible for the printed material included in this paper.